Palaeogeography, Palaeoclimatology, Palaeoecology 492 (2018) 92–103

Contents lists available at ScienceDirect

Palaeogeography, Palaeoclimatology, Palaeoecology

journal homepage: www.elsevier.com/locate/palaeo

Stable isotope ecology ($\delta^{18}O$, $\delta^{13}C$, $\delta^{15}N$) of modern land snails along an altitudinal gradient in southern Appalachian Mountains, USA

Yurena Yanes[a,*], Gary R. Graves[b,c], Christopher S. Romanek[d]

[a] Department of Geology, University of Cincinnati, Cincinnati, OH 45221, United States
[b] Department of Vertebrate Zoology, MRC-116, National Museum of Natural History, P.O. Box 37102, Smithsonian Institution, Washington, DC 20013-7012, United States
[c] Center for Macroecology, Evolution, and Climate, National Museum of Denmark, University of Copenhagen, Denmark
[d] Department of Earth and Environmental Sciences, Furman University, Greenville, SC 29613, United States

ARTICLE INFO

Keywords:
Terrestrial gastropods
Carbonate shell
Organic matter
Woodland ecosystem
Big Santeetlah Creek

ABSTRACT

The first isotopic baseline is established for the snail *Neohelix* from the Big Santeetlah Creek watershed (Appalachian Mountains). Shell $\delta^{18}O$ (−3.6 to +0.4‰) declined with altitude 0.06‰ per 100 m and correlated with measured rain $\delta^{18}O$. A flux balance model suggests that relative humidity increased from ~0.89 at 710 m to ~0.91 at 1620 m, in agreement with higher precipitation at higher altitudes. Coherent relationships between shell, precipitation and humidity suggest that this taxon should be a valid paleoprecipitation archive in North America. The respective $\delta^{13}C$ and $\delta^{15}N$ values of body (−28.3 to −23.2‰; +0.4 to +4.9‰) and shell organics (−28.2 to −24.0‰; +0.0 to +3.4‰) did not exhibit a trend with altitude and were uncorrelated with potential food resources. A stable isotope-mixing model suggests that *Neohelix* primarily consume fungi (~48%) and lichen (~17%), with minimal ingestion of C_3 plants. The relative contributions of different food items, however, varied in an unpredictable fashion along the altitudinal gradient. This study illustrates that even though snail foraging ecology from woodlands is complex and more variable than anticipated, combining several isotope systems permits dietary inferences more easily than field observations alone.

1. Introduction

Land snails are a key component of many terrestrial ecosystems where they are important agents of nutrient and biogeochemical cycling. Such biological-environmental processes are potentially recorded in the isotopic composition of land snail shells and tissues. In particular, the stable isotope composition of the shell of land snails, which are often well-preserved in the Quaternary sedimentary record, has been used as a tool for paleoenvironmental and paleoclimatic studies (e.g., Yapp, 1979; Goodfriend, 1991; Goodfriend and Ellis, 2002; Balakrishnan et al., 2005b; Colonese et al., 2007, 2010a, 2010b, 2011; Yanes et al., 2011a, b, 2012, 2013a, 2013b, 2014; Kehrwald et al. 2010; Prendergast et al., 2016). The stable isotope composition of snail organic tissues can also be used to learn aspects of snail foraging ecology (DeNiro and Epstein, 1978; Stott, 2002; Metref et al., 2003; Yanes et al., 2013c; Prendergast et al., 2017). This can be particularly valuable for many snail species with unknown ecology or unidentified dietary habits. Moreover, in the case of snail species that live in forested areas, where the trophic relationships of snails with the environment and other organisms may be difficult to understand simply through field observations, stable isotope systematics can be a significantly powerful tool (Meyer and Yeung, 2011).

Field studies on modern snails indicate that the oxygen isotopic composition ($\delta^{18}O$) of shell carbonate is related to both temperature and the $\delta^{18}O$ values of the local environmental water imbibed or absorbed through the skin of the snail (e.g., Lécolle, 1985; Goodfriend, 1991; Zanchetta et al., 2005; Yanes et al., 2008, 2009; Prendergast et al., 2015). The evaporative steady-state flux balance model proposed by Balakrishnan and Yapp (2004) suggests that the $\delta^{18}O$ of aragonite is influenced by at least four environmental variables, including relative humidity, temperature, and the $\delta^{18}O$ of precipitation and water vapor. The $\delta^{18}O$ values of the aragonitic shell, hence, may be a useful indicator of past atmospheric conditions relevant to paleoclimatic studies.

Controlled laboratory experiments suggest that the carbon isotope composition ($\delta^{13}C$) of snail shell carbonate reflects mostly respired CO_2 derived from metabolized plant material (e.g., Stott, 2002; Metref et al., 2003; Liu et al., 2007). In carbonate-rich areas, however, snails may incorporate limestone as a source of calcium to build their shells (Goodfriend and Hood, 1983; Goodfriend, 1999; Goodfriend et al., 1999; Yanes et al., 2008). For some small to minute snail species,

* Corresponding author.
E-mail address: yurena.yanes@uc.edu (Y. Yanes).

https://doi.org/10.1016/j.palaeo.2017.12.015
Received 1 August 2017; Received in revised form 8 December 2017; Accepted 15 December 2017
Available online 18 December 2017
0031-0182/

however, limestone intake seems negligible (Pigati et al., 2010). Most published investigations of modern and fossil land snails work under the assumption that they are generalized herbivores that primarily consume vascular plants (C_3, C_4 and CAM plant type) in relation to their abundance in the landscape (e.g., Goodfriend and Ellis, 2000, 2002; Baldini et al., 2007; Yanes et al., 2008, 2009, 2013c; Prendergast et al., 2017). Snail shell $\delta^{13}C$ has been traditionally used to deduce variations in C_3/C_4-CAM plants in the landscape. In C_3-plant dominated landscapes, snail $\delta^{13}C$ has also been used to infer water stress (water use efficiency) of consumed plants (e.g., Colonese et al., 2007, 2010a, 2010b, 2011; Yanes et al., 2011b, 2012, 2014; Yanes, 2015; Prendergast et al., 2017).

Shell organics, broadly defined as the protein-rich matrix in which shell carbonate crystals are embedded, constitute ~0.1% (by weight) of the shell and originate primarily from amino acids derived from the diet (e.g., Goodfriend, 1988; Goodfriend and Ellis, 2000). Similarly, snail body isotopic composition is derived from consumed foods (e.g., DeNiro and Epstein, 1978; Stott, 2002). Thus, $\delta^{13}C$ of snail organic tissues (both body and shell organics) should be, in theory, directly associated with the signature of the local vegetation, and should be a valid proxy for snail diet (e.g., DeNiro and Epstein, 1978; Goodfriend and Ellis, 2000; Yanes et al., 2008, 2009, 2013c; Prendergast et al., 2017). Less attention has been focused on the nitrogen isotope composition ($\delta^{15}N$) of land snail organic tissues, although it seems that $\delta^{15}N$ can be used to define trophic relationships among coexisting land snail species in forested habitats (Meyer and Yeung, 2011). For the particular case of herbivore snails, the organic matter $\delta^{15}N$ should therefore reflect the $\delta^{15}N$ signal of the ingested food resources after trophic fractionation correction.

In this study, we investigate three isotope systems ($\delta^{18}O$, $\delta^{13}C$, $\delta^{15}N$) of the woodland land snail *Neohelix major* morphotype, collected along an altitudinal transect (710–1620 m above sea level) in the southern Appalachian Mountains (western North Carolina, USA). We present here the first land snail study that investigates three isotope systems jointly. This research evaluates the validity of shell $\delta^{18}O$ of *Neohelix* as a paleoprecipitation proxy in North America, assesses the dietary habits of the target species in this woodland ecosystem using $\delta^{13}C$ and $\delta^{15}N$ values, and determines if shell $\delta^{13}C$ reflects the signature of dominant C_3 plants in the forest. Because this species has not been previously investigated isotopically and its ecology is minimally known, the results from this study are relevant for ecologists interested in tracing isotopically the trophic interactions among terrestrial malacofaunas in moist forest ecosystems. The result are equally relevant for paleontologists and archeologists interested in using the geochemical signature extracted from fossil shelly assemblages of *Neohelix* to reconstruct the environmental conditions of past woodland ecosystems in North America.

2. Methodology

2.1. Environmental setting

The Big Santeetlah Creek watershed (latitude: 35°21′ N; longitude: 84° 00′ W) is located on the east-facing slope of the Unicoi Mountains, within the southern Appalachian Mountains, in Graham County, North Carolina, USA (Fig. 1). The watershed, which is dominated by C_3 plant species, is cloaked in deciduous and mixed deciduous-coniferous forest ranging in altitude from 680 to 1689 m (Graves et al., 2002; Graves and Romanek, 2009). C_3 grassland is present on a few peaks above 1600 m. C_4 agricultural crops have not been cultivated in the watershed since the 1930s (Graves et al., 2002).

The local climate is characterized by mild summers with cool nights and relatively high precipitation rates. Winters are also mild but with periods of colder temperatures and snow. At higher altitudes (> 1600 m), temperatures fluctuate strongly throughout the year and precipitation is more intense and frequent than at lower sites. Mean minimum and maximum temperatures decrease with increasing altitude ~0.3–0.7 °C per 100 m (e.g., Bolstad et al., 1998). Mean monthly temperatures on east facing slopes vary from −3 °C to 6 °C in winter and from 17 °C to 26 °C in summer (see Fig. 1 in Bolstad et al., 1998). The Big Santeetlah Creek watershed is a humid area with annual precipitation varying from ~1100 mm to ~1600 mm depending on altitude.

2.2. Sampling strategy

2.2.1. Water

Rain samples (n = 42) were collected at eight sampling sites (Table S1; Table 1) to estimate the $\delta^{18}O$ of the local meteoric water along the altitudinal gradient: (1) Santeetlah Bridge (710 m), (2) Rhododendron (800 m), (3) Graves' camp (845 m), (4) Sand Creek (910 m), (5) Cold Branch (1010 m), (6) Whigg Branch (1135 m), (7) Stratton Gap (1310 m) and (8) Hooper Bald (1620 m). The direct line distance from Santeetlah Bridge (710 m) to Hooper Bald (1620 m) was 9.0 km. Several sample replicates were collected per site during February and October of 2001 and 2002. Samples were gathered in 12 ml plastic bottles at the moment of the rainfall event and sealed immediately to prevent evaporation.

2.2.2. Plants

Vascular plant samples (n = 187) were collected at eight localities along the altitudinal gradient (Table S2; Table 2). Three tree species were selected for study based on their abundance/dominance in the landscape: eastern hemlock (Pinaceae: *Tsuga canadensis*), yellow birch (Betulaceae: *Betula alleghaniensis*) and rosebay rhododendron (Ericaceae: *Rhododendron maximum*). A mixture of new and older leaves from each species was collected at each sampling site for bulk isotopic analysis. Collected leaves included those exposed to full sunlight and those under constant shade. In addition, eight duff samples (decaying leaves and other plant material on the soil surface) and 36 humus samples (decayed organic matter present in the upper few centimeters of the soil profile) were gathered as grab samples for subsequent bulk analysis. Care was taken to avoid depressions (relatively wet areas) and mounds (relatively dry areas) to minimize variation in soil water saturation.

We also collected and analyzed samples of fungi, lichen and moss from each site. Taxonomic identifications of these specimens were not possible. Multiple individuals and species were gathered per site when available and accessible. We assume that computed average isotopic values for each of these taxonomic groups should be reasonably representative of these potential food resources. Collectively, these samples provide an estimate of the $\delta^{13}C$ and $\delta^{15}N$ profiles of the dominant vegetation and fungi in the study area.

2.2.3. Land snails

Living snails (n = 55) were collected from 2003 to 2005 at the eight localities along the altitudinal transect (Table S3; Table 3). On the basis of shell characteristics, these had been identified as *Neohelix albolabris* (Say, 1817) (Gastropoda: Polygyridae), a herbivorous pulmonate snail (with occasional omnivore behavior) that grazes on or near the forest floor. However, this taxon has been determined to represent a complex of cryptic allopatric species (Emberton, 1988, 1995). Populations from the southern Appalachian Mountain are now referred to as *Neohelix major* (A. Binney, 1837), commonly known as the “southeastern whitelip”. Taxonomic classification is further complicated by the convergence of shell characters of *N. major* and *Mesodon normalis* (Pilsbry, 1900), which are sympatric and overlap attitudinally in many locations in the southern Appalachian Mountains (Emberton, 1994, 1995). These taxa can be reliably distinguished morphologically by genital characters (Emberton, 1994, 1995) and molecular markers, neither of which were examined in all our specimens. Thus our population sample of *N. major* morphotypes could contain both taxa. However, because the two taxa exhibit morphological convergence in natural sympatry (Emberton,

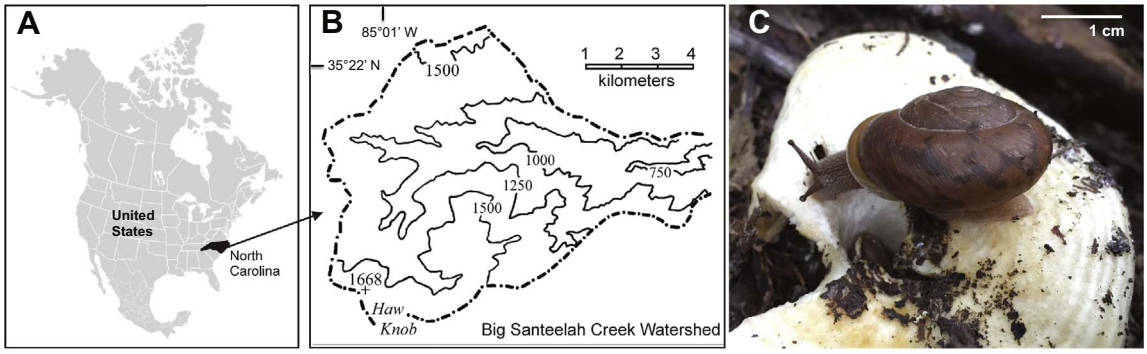

Fig. 1. (A–B) Geographical location of the Big Santeetlah Creek watershed sampling site, indicating the altitudinal gradient sampled (in meters) in western North Carolina (Adapted after Graves et al. 2002). (C) Field photograph of *Neohelix major* morphotype feeding on fungi.

Table 1
Site-averaged (± standard deviation) of oxygen isotopes of measured precipitation and calculated mean annual precipitation (MAT) $\delta^{18}O$ values from the Online Isotopes in Precipitation Calculator (OIPC) website (http://www.waterisotopes.org).

Locality	Altitude (m)	n	Measured precipitation $\delta^{18}O$ (‰ SMOW)	Calculated MAT $\delta^{18}O$ (‰ SMOW)
Santeetlah Bridge	710	6	−5.6 ± 0.3	−6.7
Rhododendrom	800	6	−5.5 ± 0.1	−6.9
Graves' Camp	845	6	−5.8 ± 0.2	−7.0
Sand Creek	910	6	−6.0 ± 0.2	−7.1
Cold Branch	1010	4	−6.1 ± 0.1	−7.3
Whigg Branch	1135	4	−6.0 ± 0.1	−7.6
Stratton Gap	1310	3	−6.0 ± 0.2	−8.0
Hooper Bald	1620	2	−6.3 ± 0.0	−8.7

n: number of samples analyzed.

1995) and in laboratory experiments, we assume that they are physiologically similar. The *N. major* morphotype was selected for study because it was present at all sampling sites, although its abundance varied considerably among localities. Also, its large and thick shell exhibits high durability in the archeological and fossil record. Adult individuals of the *N. major* morphotype exhibit a shell diameter of ~26.9–39.3 mm, shell height of ~16.0–17.0 mm, and whorl spire number of 5.4–6.4 (Emberton, 1995). All specimens were collected from terrestrial substrates (leaf litter, rocks, fallen logs), held for five days in plastic bags without access to food at 10 °C to assure that gut contents were voided, and then preserved in 80% ethanol.

Although specific information about *Neohelix* behavior is unknown, the majority of land snail species are known to be active at night and/or during rainy periods. Shell growth mostly occurs during periods of activity (warmest and wettest seasons of the year). Generally, land snails of temperate zones can enter in a dormant state (cease growing) when temperatures drop below ~10 °C or rise above ~27 °C (e.g., Cook, 2001). *Neohelix* is expected to become dormant from several weeks to a couple of months during the winter season, when temperatures drop significantly. We assume as a working hypothesis that the measured individuals were active and grew shell for much of the growing season (i.e., from late February to late November).

2.3. Laboratory analyses

2.3.1. Stable oxygen isotope analysis of the water

Twelve milliliters exetainers™ containing a small aliquot (< 0.2 ml) of 100% H_3PO_4 acid were flushed with 0.3% CO_2 in He to replace air in the headspace of the water sample vials. Acid was added to the water samples to lower the pH and prevent oxygen isotope fractionation between the aqueous CO_2 and other species of the dissolved inorganic carbon (DIC) such as H_2CO_3 or CO_3. Lower water pH also facilitates exchange between the oxygen isotopes in the water and aqueous CO_2, and minimizes exchange with other DIC species, which are virtually non-existent at low pH. Water (0.5 ml) was then injected through a septum into the vial and left to equilibrate at 25 °C for 48 h. The headspace was then analyzed using a Gas Bench II peripheral device connected to the Finnigan Delta^{PLUS} XL continuous flow isotope ratio mass spectrometer (CF-IRMS). Stable isotope values are reported in δ notation relative to the Standard Mean Ocean Water (SMOW). The δ values are defined as:

$$\delta^{18}O = [(R_{sample}/R_{standard})-1] \times 1000\ (‰) \quad (1)$$

where $R = {}^{18}O / {}^{16}O$. Analytical uncertainty was ± 0.1‰ based on repeated measurements of several VSMOW: Vienna-Standard Mean Ocean Water ($\delta^{18}O = +0‰$) and SLAP: Standard Light Antarctic Precipitation ($\delta^{18}O = -55.5‰$) international standards dispersed throughout a run.

2.3.2. Stable nitrogen and carbon isotope analysis of the organic matter

Freshly-picked tree leaves were rinsed with distilled water and oven-dried at 40 °C for 48 h. We focused on analyzing fresh leaves rather than other plant parts (e.g., stems) because we assume than snails would preferentially consume the softer parts of the plants. Samples of fungi, moss, and lichen were rinsed with distilled water and dried overnight at room temperature. Dried samples were then ground finely using an electric blender. Duff and humus samples were treated with 2 M HCl overnight at room temperature to remove possible carbonate minerals. Samples were then rinsed with deionized water and oven-dried at 40 °C for 48 h.

The soft snail body was separated manually from the shell, rinsed with deionized water, oven-dried at 40 °C overnight and homogenized using an electric blender. The shell organic matter was extracted from each homogenized shell by placing the shell in a beaker with 2 M HCl solution at room temperature until the shell carbonate fully dissolved (several hours). A small aliquot of the pulverized pre-treated shell was saved for carbonate isotopic analysis. The organic matter, which included the periostracum and both the acid soluble and insoluble organic matrix of the shell, was recovered as a pellet after centrifugation, rinsed with deionized water, and oven dried at 40 °C overnight.

Organic samples preserved in ethanol do not vary considerably in $\delta^{15}N$ with respect to the original tissue whereas the $\delta^{13}C$ may vary as a consequence of resulting lipid extraction, particularly in fat-rich tissues (e.g., Hobson et al., 1997; Sarakinos et al., 2002; Sweeting et al., 2004; Barrow et al., 2008). Land snail body tissue is rich in protein (> 15–30% by weight) and poor in fat content (< 2–4% by weight) (e.g., Lubell, 2005 and references therein). This was confirmed by a preliminary laboratory test, which indicated that lipid-extracted and non-lipid extracted snail body samples yielded similar $\delta^{13}C$ values (offsets between treated and non-treated samples were lower than ~0.2‰; n = 10). Consequently, the preservation method employed here for land snail samples should have not affected substantially the

Table 2
Site-averaged (± standard deviation) of carbon and nitrogen isotopes of potential snail foods.

		Tsuga (Pinaceae)			Rhododendron (Ericaceae)		
Locality	Altitude (m)	n	$\delta^{13}C$	$\delta^{15}N$	n	$\delta^{13}C$	$\delta^{15}N$
Santeetlah Bridge	710	7	− 29.9 ± 1.2	− 2.5 ± 0.2	7	− 29.6 ± 2.1	− 3.0 ± 0.7
Rhododendrom	800	6	− 29.4 ± 0.7	− 1.3 ± 0.3	6	− 30.3 ± 1.1	− 3.6 ± 0.9
Graves' Camp	845	5	− 29.7 ± 0.9	− 2.5 ± 1.3	6	− 30.3 ± 1.5	− 2.7 ± 1.2
Sand Creek	910	7	− 29.1 ± 0.9	− 1.1 ± 1.1	7	− 30.6 ± 1.1	− 2.9 ± 0.9
Cold Branch	1010	7	− 29.7 ± 0.6	− 2.3 ± 0.8	6	− 29.3 ± 1.4	− 2.4 ± 0.7
Whigg Branch	1135	7	− 29.0 ± 0.7	− 1.9 ± 0.7	6	− 29.5 ± 1.4	− 3.6 ± 0.8
Stratton Gap	1310	7	− 28.0 ± 1.1	− 2.2 ± 1.0	6	− 29.2 ± 1.3	− 2.9 ± 0.8
Hooper Bald	1620	7	− 26.6 ± 0.6	− 0.2 ± 0.7			

		Betula (Betulaceae)			Duff		
Locality	Altitude (m)	n	$\delta^{13}C$	$\delta^{15}N$	n	$\delta^{13}C$	$\delta^{15}N$
Santeetlah Bridge	710	5	− 30.7 ± 0.9	− 0.1 ± 1.8	1	− 28.8	− 1.7
Rhododendrom	800	4	− 29.2 ± 0.7	− 4.3 ± 0.7	1	− 28.0	− 1.5
Graves' Camp	845	5	− 30.2 ± 1.2	− 1.1 ± 1.7	1	− 28.2	− 2.0
Sand Creek	910	5	− 31.0 ± 1.0	− 1.8 ± 1.2	1	− 29.2	− 2.6
Cold Branch	1010	5	− 30.0 ± 1.6	− 1.7 ± 1.3	1	− 28.3	− 0.8
Whigg Branch	1135	5	− 30.6 ± 1.1	− 0.7 ± 1.4	1	− 28.4	− 1.3
Stratton Gap	1310	5	− 29.8 ± 1.6	− 0.9 ± 0.6	1	− 27.4	− 1.8
Hooper Bald	1620	5	− 28.5 ± 0.8	− 1.6 ± 1.0	1	− 26.7	+ 0.1

		Humus			Fungi		
Locality	Altitude (m)	n	$\delta^{13}C$	$\delta^{15}N$	n	$\delta^{13}C$	$\delta^{15}N$
Santeetlah Bridge	710	4	− 28.3 ± 0.4	− 0.3 ± 1.1	2	− 26.0 ± 0.3	− 0.4 ± 4.7
Rhododendrom	800	4	− 27.6 ± 0.3	− 0.9 ± 1.1	3	− 24.9 ± 3.0	+ 0.5 ± 2.2
Graves' Camp	845	3	− 27.8 ± 0.4	− 1.5 ± 1.6	4	− 23.6 ± 1.2	− 1.4 ± 2.6
Sand Creek	910	6	− 27.8 ± 0.9	− 0.3 ± 1.5	2	− 24.4 ± 0.0	+ 3.2 ± 6.6
Cold Branch	1010	5	− 27.8 ± 0.7	− 0.2 ± 1.1	2	− 24.8 ± 0.8	+ 0.0 ± 2.0
Whigg Branch	1135	5	− 28.0 ± 0.7	− 0.1 ± 1.2	2	− 23.5 ± 0.3	+ 1.2 ± 0.5
Stratton Gap	1310	5	− 27.7 ± 0.3	− 1.2 ± 2.0	4	− 23.4 ± 0.8	− 0.9 ± 2.1
Hooper Bald	1620	4	− 26.9 ± 0.5	+ 0.6 ± 1.1	3	− 22.3 ± 0.8	+ 0.9 ± 2.7

		Lichen			Moss		
Locality	Altitude (m)	n	$\delta^{13}C$	$\delta^{15}N$	n	$\delta^{13}C$	$\delta^{15}N$
Santeetlah Bridge	710	2	− 25.0 ± 0.6	− 9.5 ± 2.7	2	− 31.1 ± 0.3	− 3.7 ± 0.5
Rhododendrom	800	4	− 24.2 ± 1.3	− 8.6 ± 3.3	3	− 29.8 ± 1.7	− 3.1 ± 0.3
Graves' Camp	845	2	− 25.3 ± 2.3	− 7.8 ± 5.3	1	− 28.8	− 4.5
Sand Creek	910	1	− 23.8	− 7.7	1	− 30.1	− 4.2
Cold Branch	1010	2	− 24.1 ± 0.8	− 10.4 ± 3.6	1	− 26.2	− 5.6
Whigg Branch	1135	2	− 22.9 ± 2.5	− 8.7 ± 1.0	1	− 29.4	− 5.3
Stratton Gap	1310	2	− 22.5 ± 0.1	− 9.9 ± 1.4	1	− 30.9	− 3.9
Hooper Bald	1620	5	− 25.2 ± 4.8	− 4.7 ± 3.6	2	− 26.4 ± 0.4	− 4.3 ± 1.2

n: number of samples analyzed.

Table 3
Site-averaged (± standard deviation) of carbon, nitrogen and oxygen isotopes of land snail shell and tissue.

Locality	n	Altitude (m)	Body		Shell organics		Shell carbonate	
			$\delta^{13}C$	$\delta^{15}N$	$\delta^{13}C$	$\delta^{15}N$	$\delta^{13}C$	$\delta^{18}O$
Santeetlah Bridge	3	710	− 25.7 ± 0.8	+ 2.2 ± 0.7	− 26.4 ± 1.0	+ 1.5 ± 1.5	− 11.8 ± 0.9	− 1.5 ± 0.7
Rhododendron	8	800	− 25.1 ± 0.7	+ 1.2 ± 0.2	− 25.5 ± 0.7	+ 0.9 ± 0.4	− 10.7 ± 1.3	− 1.8 ± 1.2
Graves' Camp	6	845	− 24.0 ± 0.3	+ 2.2 ± 1.4	− 24.6 ± 0.4	+ 0.8 ± 0.6	− 9.7 ± 1.2	− 1.4 ± 0.5
Sand Creek	7	910	− 24.9 ± 0.8	+ 2.3 ± 1.6	− 25.0 ± 0.8	+ 1.5 ± 1.4	− 11.6 ± 2.0	− 1.9 ± 0.8
Cold Branch	8	1010	− 26.3 ± 0.6	+ 2.0 ± 1.0	− 26.9 ± 0.5	+ 1.3 ± 0.7	− 11.5 ± 0.8	− 2.1 ± 0.7
Whigg Branch	9	1135	− 25.4 ± 1.3	+ 1.2 ± 0.6	− 25.2 ± 1.3	+ 1.0 ± 0.5	− 11.7 ± 2.1	− 1.8 ± 0.8
Stratton Gap	6	1310	− 25.3 ± 1.7	+ 1.5 ± 0.7	− 25.9 ± 1.5	+ 1.1 ± 0.8	− 11.0 ± 0.8	− 2.0 ± 0.8
Hooper Bald	8	1620	− 25.4 ± 0.6	+ 1.4 ± 0.5	− 26.0 ± 0.8	+ 1.2 ± 0.3	− 11.5 ± 2.2	− 2.1 ± 0.8

n: number of samples analyzed.

$\delta^{13}C$ and $\delta^{15}N$ values of the original tissues. Moreover, potential effects of ethanol should have affected equally all analyzed samples because they all were preserved using the same method.

Between 1.0 and 1.5 mg of organic matter was weighed into a tin capsule, crimped, and combusted in a Carlo Erba Elemental Analyzer (NC 2500). The CO_2 and N_2 produced after combustion were analyzed in the CF-IRMS. Stable isotope results are reported in δ notation relative to Pee Dee Belemnite (PDB) for carbon isotopes and air for nitrogen isotopes. Analytical uncertainty for both isotopes was ± 0.1‰ based on the repeated measurements of several in-house standards: (1) DORM 3 (NRC Canada dogfish muscle): $\delta^{13}C = -19.6‰$ and $\delta^{15}N = +12.5‰$; (2) ACE (Acetanilide from Thermo Fisher): $\delta^{13}C = -29.3‰$ and $\delta^{15}N = -0.4‰$; and (3) CCHICK (lipid extracted chicken feathers from Athens, GA): $\delta^{13}C = -16.4‰$ and $\delta^{15}N = +3.2‰$; dispersed periodically throughout a run sequence (n = 15). Reproducibility of replicate samples was generally better than ± 0.2‰ (n = 3) for $\delta^{15}N$ and $\delta^{13}C$.

2.3.3. Stable oxygen and carbon isotope analysis of the shell carbonate

Small aliquots of each pre-cleaned and finely ground whole shell were treated with 3% NaOCl (reagent grade) overnight at room temperature (~22 °C) to remove organic contaminants and shell organic matter. Previous laboratory tests indicated that NaOCl-treated and untreated shell exhibit equivalent carbon and oxygen isotope values (< 0.2‰). About 150 μg of carbonate powder was placed in a 6 ml Exetainer™ vial that was subsequently flushed with helium to replace the headspace. The carbonate was then converted to CO_2 gas by adding 0.1 ml of 100% H_3PO_4 at 25 °C. The resulting CO_2 was analyzed after 24 h using the GasBench II connected to the CF-IRMS. Stable isotope results are reported in δ notation relative to Pee Dee Belemnite (PDB) for both carbon and oxygen isotopes. Analytical uncertainty was ± 0.1‰ based on the repeated measurements of the international standard NBS-19 ($\delta^{13}C = +1.95‰$ and $\delta^{18}O = -2.20‰$) throughout a run (n = 24). Reproducibility of sample replicates was generally better than ± 0.2‰ (n = 5) for both $\delta^{13}C$ and $\delta^{18}O$.

Water, vascular plants and snail samples were all prepared and analyzed in the Savannah River Ecology laboratory (SREL) of the University of Georgia (UGA) whereas fungi, moss and lichen samples were prepared at the University of Cincinnati (UC) and analyzed in the Stable Isotope Facility of the University of New Mexico (UNM).

2.4. Statistical treatment

All statistical analyses were performed using *PAST 3.12* software (Hammer et al., 2001) considering statistical significance at $\alpha = 0.05$. Due to the uneven number of samples of different organisms per site, and because we wanted to evaluate the relationship among variables along an altitudinal gradient, we contrasted site-averaged data rather than raw data. Because of the limited number of sampling sites (eight localities along the altitudinal gradient) we used Spearman correlation coefficients to measure the strength of monotonic association between two ranked variables. Ordinary least square regression was employed for site-averaged data (n = 8) to estimate the slope and intercept of the potential linear relationships between variables. Pearson correlation p-values are included together with linear regression equations in figures.

2.5. Land snail flux balance mixing models

Balakrishnan and Yapp (2004) developed a simple steady-state flux balance-mixing model to interpret the aragonitic shell $\delta^{13}C$ and $\delta^{18}O$ of land snails. These models optimize the information that can be extracted from the shell carbonate precipitated during snail growth in a quantitative manner. The $\delta^{18}O$ model establishes (1) a quantitative relationship between the amount and isotopic composition of liquid water imbibed or absorbed by the snails, (2) the amount and isotopic composition of liquid water from the snail body fluid, (3) the diffusive flux of water from the body fluid by evaporation, and (4) the temperature dependent oxygen isotope fractionation between the body fluid and aragonite shell (Grossman and Ku, 1986). The model posits that temperature, $\delta^{18}O$ of water and water vapor, and relative humidity are the most important variables in the accurate determination of the body fluid and the shell $\delta^{18}O$ (Balakrishnan and Yapp, 2004). Another important parameter is the flux of liquid water output from the body fluid (f_o) relative to the flux of liquid water ingested by the snail (f_{in}) during shell formation (i.e., when the snail is active). This ratio is called θ, which is defined as $\theta = (f_o/f_{in})$. Balakrishnan and Yapp (2004) showed that it is appropriate, in many instances, to assume that ambient water vapor is in isotope equilibrium with the imbibed or adsorbed liquid water (see also Yanes et al. 2011a). Furthermore, for $\theta \leq 0.40$, an assumption that snail body fluid is lost only by evaporation (i.e., $\theta = 0$) is a good approximation and introduces very little error in model calculations (Balakrishnan and Yapp, 2004). Thus, a value of $\theta = 0$ is adopted here. Model calculations are also constrained by the use of the measured shell carbonate $\delta^{18}O$, the mean ambient temperature when snails deposited shell (~20 °C at 710 m and ~16 °C at 1620 m), and the measured $\delta^{18}O$ of rainfall: −5.6 (‰ SMOW) at 710 m and −6.3 (‰ SMOW) at 1620 m.

For $\delta^{13}C$, the model builds a quantitative relationship between the amount and isotopic composition of plants consumed by snails, the amount and isotopic composition of bicarbonate generated in the snail body fluid, and the diffusive flux of CO_2 gas from the snail body fluid. Another parameter that arises in the model is the flux of bicarbonate output from the body fluid (f_o) relative to the flux of input bicarbonate arising from metabolic oxidation of dietary items consumed by the snail (f_{in}) during the shell mineralization process (i.e., when the snail is feeding). This ratio is called Φ, defined as $\Phi = (f_o/f_{in})$, which varies with metabolic rate (see Balakrishnan and Yapp, 2004 for further details). Model calculations are constrained by the use of the measured $\delta^{13}C$ values for shell carbonate and organic matter tissues (i.e., plants, snail body, shell organics) and the mean ambient temperature during shell morphogenesis. We parameterized the model by assuming an ambient temperature of ~20 °C in our study area, but it has been shown that variance in temperature of calcification has a minor effect on the model output (Balakrishnan and Yapp, 2004). We also assumed that snails deposited shell carbonate from dietary sources obtained ultimately from C_3 plants.

2.6. Dietary reconstruction via IsoSource

Contributions of potentially consumed food resources by snails (in this study, C_3 plants, duff, humus, fungi, moss, and lichen) were computed using the *IsoSource 1.3.1* software (https://www.epa.gov/eco-research/stable-isotope-mixing-models-estimating-source-proportions) (Phillips and Gregg, 2003), which is consistent with isotopic mass balances. This model computes the range of feasible source contributions to a mixture when there are too many sources to allow a unique solution through isotopic signatures (Phillips and Gregg, 2003; Newsome et al. 2004; Phillips and Newsome, 2015). All possible combinations of each source contribution (0–100%) are examined in small increments (in this study, 2%). Combinations that sum to the observed mixture of isotopic signatures within a small tolerance (in this study, ± 0.1‰) are considered feasible solutions, from which the frequency and range of potential source contributions can be determined (Phillips and Gregg, 2003; Newsome et al., 2004; Phillips et al., 2015). The mean carbon and nitrogen isotope values of all measured snail body tissues (n = 55) were adjusted for trophic fractionation before analysis to 0.4‰ and 3.4‰ for carbon and nitrogen, respectively (Post, 2002).

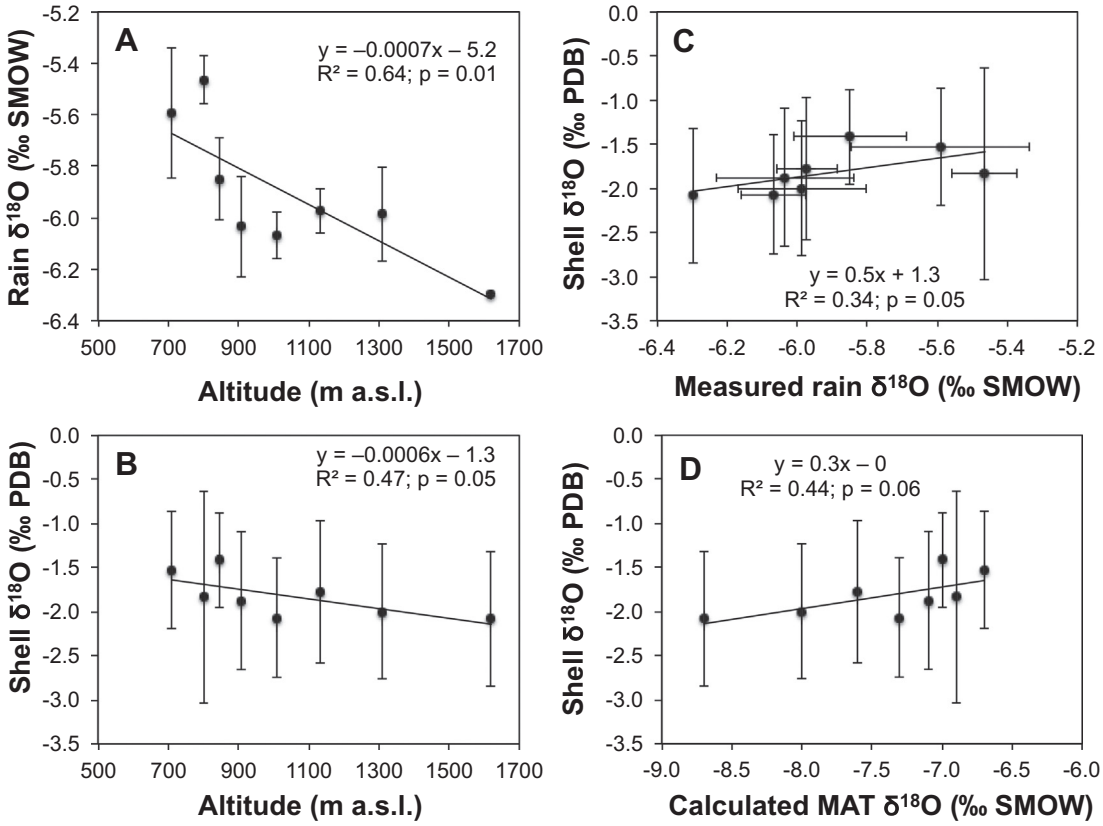

Fig. 2. Oxygen stable isotope values of precipitation and land snail shells along an altitudinal gradient in the Big Santeetlah Creek watershed. (A) Measured precipitation $\delta^{18}O$. (B) Shell carbonate $\delta^{18}O$. (C) Relationship between $\delta^{18}O$ of measured precipitation and shell carbonate. (D) Relationship between $\delta^{18}O$ of calculated mean annual precipitation and shell carbonate. Filled symbols represent mean values and whiskers represent 1σ standard deviation. Solid lines represent the regression line of the data.

3. Results

3.1. Rainwater $\delta^{18}O$

The $\delta^{18}O$ values for individual rain events from the Big Santeetlah Creek watershed ranged from −6.3‰ to −5.2‰ (Table S1) and declined significantly with increasing altitude (Fig. 2A). The $\delta^{18}O$ of rain samples collected in February and October were not significantly different. The lapse rate of site-averaged rain $\delta^{18}O$ was ~0.07‰ per 100 m (n = 8) (Table 1; Fig. 2A). The $\delta^{18}O$ of calculated mean annual precipitation (MAP) from the Online Isotopes in Precipitation Calculator (OIPC; (http://www.waterisotopes.org) were 1.1 to 2.4‰ lower than measured rain samples from the Big Santeetlah Creek watershed (Table 1). Calculated MAP $\delta^{18}O$ declined ~0.22‰ per 100 m increase in altitude. Lower precipitation $\delta^{18}O$ values estimated from the OIPC model are likely due to the inclusion of precipitation events with lower $\delta^{18}O$ values during the winter months.

3.2. Shell carbonate $\delta^{18}O$

The $\delta^{18}O$ of shell carbonate ranged from −3.6‰ to +0.4‰ (Table S3), with a mean value of −1.9 ± 0.8‰. Site-averaged shell $\delta^{18}O$ (Table 2) declined significantly with altitude at the rate of −0.06‰ per 100 m (Fig. 2B) and correlated positively with average $\delta^{18}O$ of the measured precipitation by site (Spearman correlation: $r_s = 0.83$; $p = 0.017$; $n = 8$) (Fig. 2C) and the calculated MAT $\delta^{18}O$ from the OIPC website (Spearman correlation: $r_s = 0.59$; $p = 0.039$; $n = 8$) (Fig. 2D). Shell $\delta^{18}O$ was uncorrelated with $\delta^{13}C$ and $\delta^{15}N$ values from plants, snail bodies, and shell organics.

The outputs of the flux balance mixing model by Balakrishnan and Yapp (2004) for shell $\delta^{18}O$ (Fig. 3) suggest that snails at 710 m, with a mean shell $\delta^{18}O$ value of −1.5 (‰ PDB), precipitated carbonate at

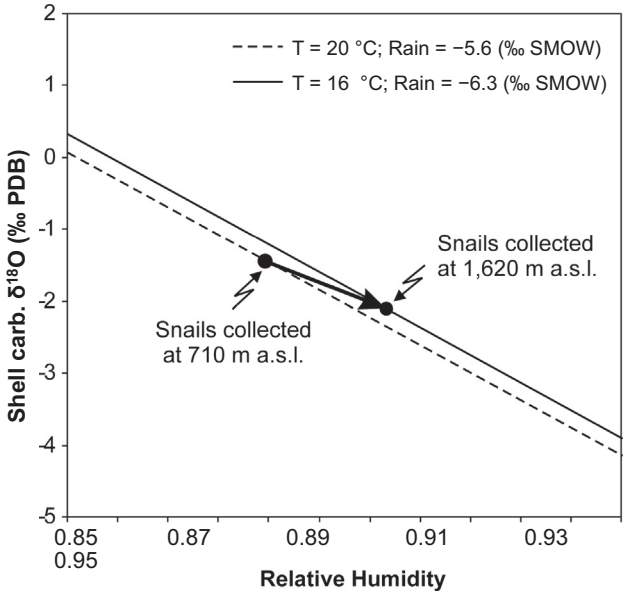

Fig. 3. Calculations of shell $\delta^{18}O$ using the snail evaporative steady-state flux balance model of Balakrishnan and Yapp (2004), assuming isotopic equilibrium between precipitation and water vapor (see text). Filled circles represent the mean measured shell $\delta^{18}O$ for snails at 710 and 1620 m. Heavy arrow depicts a hypothetical trajectory of declining shell $\delta^{18}O$ with increasing altitude, as a result of the combined effects of increasing relative humidity, declining precipitation $\delta^{18}O$ and decreasing temperature.

times when relative humidity was ~0.89, ambient temperature was ~20 °C and rain $\delta^{18}O$ was ~−5.6 (‰ SMOW). On the other hand, snails at the highest altitude locality (1620 m), with a mean shell $\delta^{18}O$

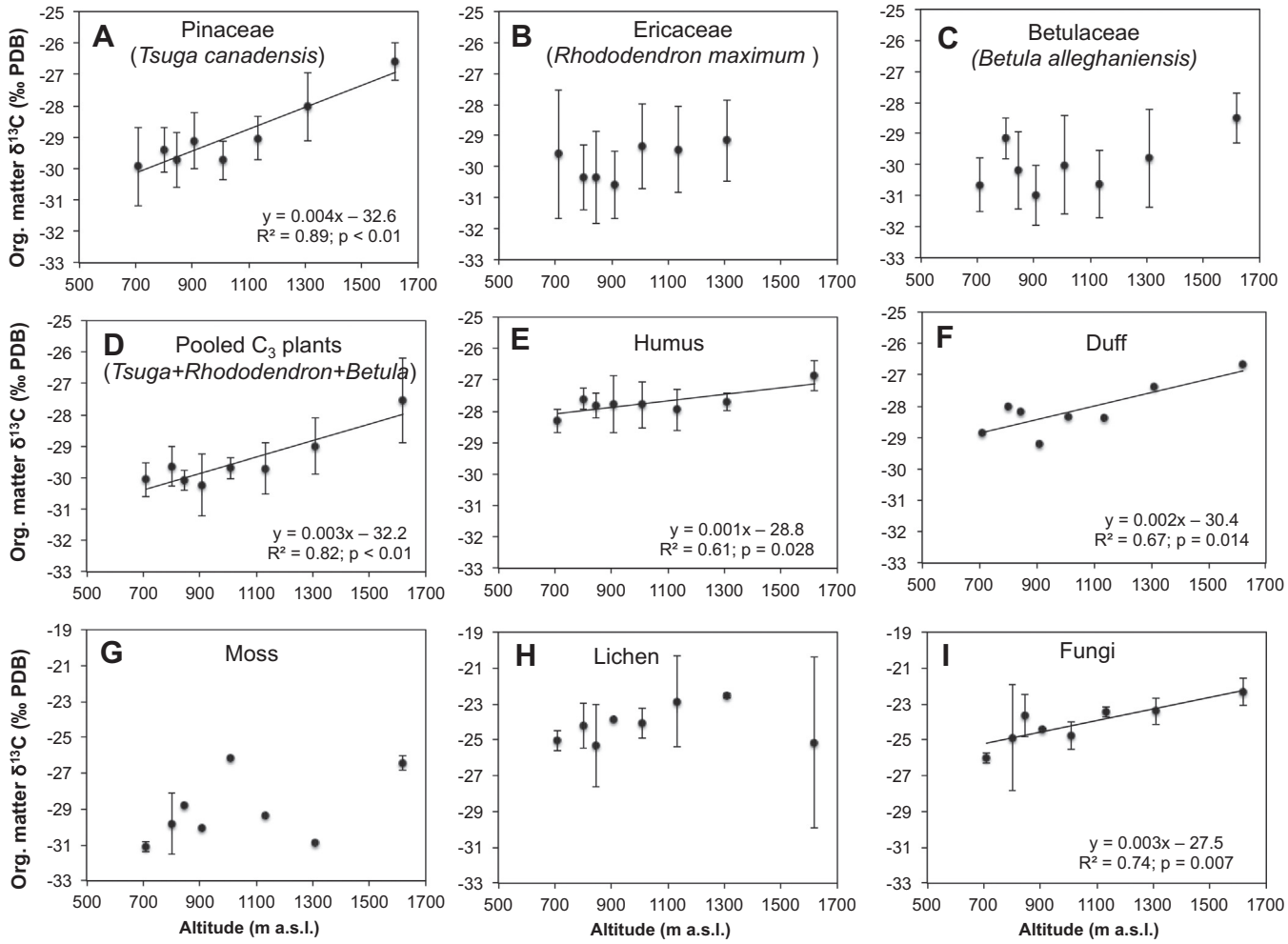

Fig. 4. Carbon stable isotopes of food resources along an altitudinal gradient in the Big Santeetlah Creek watershed. (A) $\delta^{13}C$ of *Tsuga canadensis*. (B) $\delta^{13}C$ of *Betula alleghaniensis*. (C) $\delta^{13}C$ of *Rhododendron maximum*. (D) $\delta^{13}C$ of pooled C_3 plants. (E) $\delta^{13}C$ of humus. (F) $\delta^{13}C$ of duff. (G) $\delta^{13}C$ of moss. (H) $\delta^{13}C$ of lichen. (I) $\delta^{13}C$ of fungi. Solid lines represent the regression line of the data for cases where statistical significance is reached.

of − 2.1 (‰ PDB), plausibly deposited carbonate when relative humidity was ~0.91, air temperature was ~16 °C and precipitation $\delta^{18}O$ was ~−6.3 (‰ SMOW), on average (Fig. 3). Thus, calcification at lower sites appears to have occurred under slightly drier and warmer conditions.

3.3. Potential food resources $\delta^{13}C$ and $\delta^{15}N$

The $\delta^{13}C$ of living leaves of the three C_3 tree species ranged from − 32.8‰ to − 26.2‰ (Table S2). The $\delta^{13}C$ for the coniferous *Tsuga canadensis* (Fig. 4A) increased significantly with altitude at a rate of 0.4‰ per 100 m, in agreement with lower carbon uptake by carboxylation at higher sites (Körner et al., 1988). In contrast, $\delta^{13}C$ for the deciduous tree *Betula alleghaniensis* (Fig. 4B) and the small evergreen broadleaf tree, *Rhododendron maximum* (Fig. 4C), were uncorrelated with altitude. The $\delta^{13}C$ of duff and humus varied from − 29.2‰ and − 26.3‰ (Table S2), and increased significantly with altitude at the rate of + 0.1‰ and + 0.2‰ per 100 m, respectively (Fig. 4D–E). Foliage of all tree species combined (n = 135) exhibited a mean $\delta^{13}C$ value of − 29.5‰ whereas soil organic matter (n = 43) showed a mean value of − 27.8‰ (almost ~2‰ enriched in ^{13}C compared to living plants). $\delta^{13}C$ values varied from − 28.2 to − 21.5‰ in fungi (n = 22), − 30.4 to − 20.5‰ in lichen (n = 20) and − 31.3 to − 26.1‰ in moss (n = 12)(Table S2). While $\delta^{13}C$ increased 0.3‰ per 100 m in fungi (Fig. 4I), it did not vary systematically with altitude for lichen (Fig. 4H) and moss (Fig. 4G).

The $\delta^{15}N$ of fresh tree leaves ranged from − 5.2‰ to + 1.6‰ (Table S2). The foliar $\delta^{15}N$ of *Tsuga canadensis* (Fig. 5A), *Betula alleghaniensis* (Fig. 5B), and *Rhododendron maximum* (Fig. 5C) did not vary with altitude. $\delta^{15}N$ of bulk soil organic matter samples varied from − 4.7‰ to + 2.2‰ (Table S2), but neither duff (Fig. 5D) nor humus (Fig. 5E) showed a trend with altitude. Fresh plant tissue (n = 135) exhibited a mean $\delta^{15}N$ value of − 2.1‰ whereas bulk soil organic matter (n = 43) displayed a mean value of − 0.6‰ (~1.5‰ higher than living vascular plant matter). The $\delta^{15}N$ of fungi (n = 22), lichen (n = 20) and moss (n = 12) varied between − 4.8 and + 7.8‰; − 13.0 and − 0.8‰; and − 5.6 and − 2.8‰, respectively (Table S2). As with vascular plant samples, the $\delta^{15}N$ of fungi (Fig. 5I), lichen (Fig. 5H) and moss (Fig. 5G) did not vary predictably with altitude.

3.4. Land snail organic tissues $\delta^{13}C$ and $\delta^{15}N$

The $\delta^{13}C$ of snail body (n = 55) ranged from − 28.3‰ to − 23.2‰ (Table S3), with a mean value of − 25.3 ± 1.1‰. Body $\delta^{13}C$ did not vary significantly with altitude (Fig. 6A; Table 2). The $\delta^{13}C$ of shell organics ranged from − 28.2‰ to − 24.0‰ (Table S3), and showed a mean value of − 25.7 ± 1.1‰. Shell organic matter $\delta^{13}C$ did not exhibit a trend with altitude either (Fig. 6B; Table 2). The site-averaged $\delta^{13}C$ values of snail body and shell organics were correlated (Spearman correlation: r_s = 0.90; p = 0.005; n = 8; Fig. 6D) but both were uncorrelated with mean $\delta^{13}C$ values of food resources per site. The carbon isotopic offset between snail body and C_3 plant ($\Delta^{13}C_{body\text{-}plant}$) within

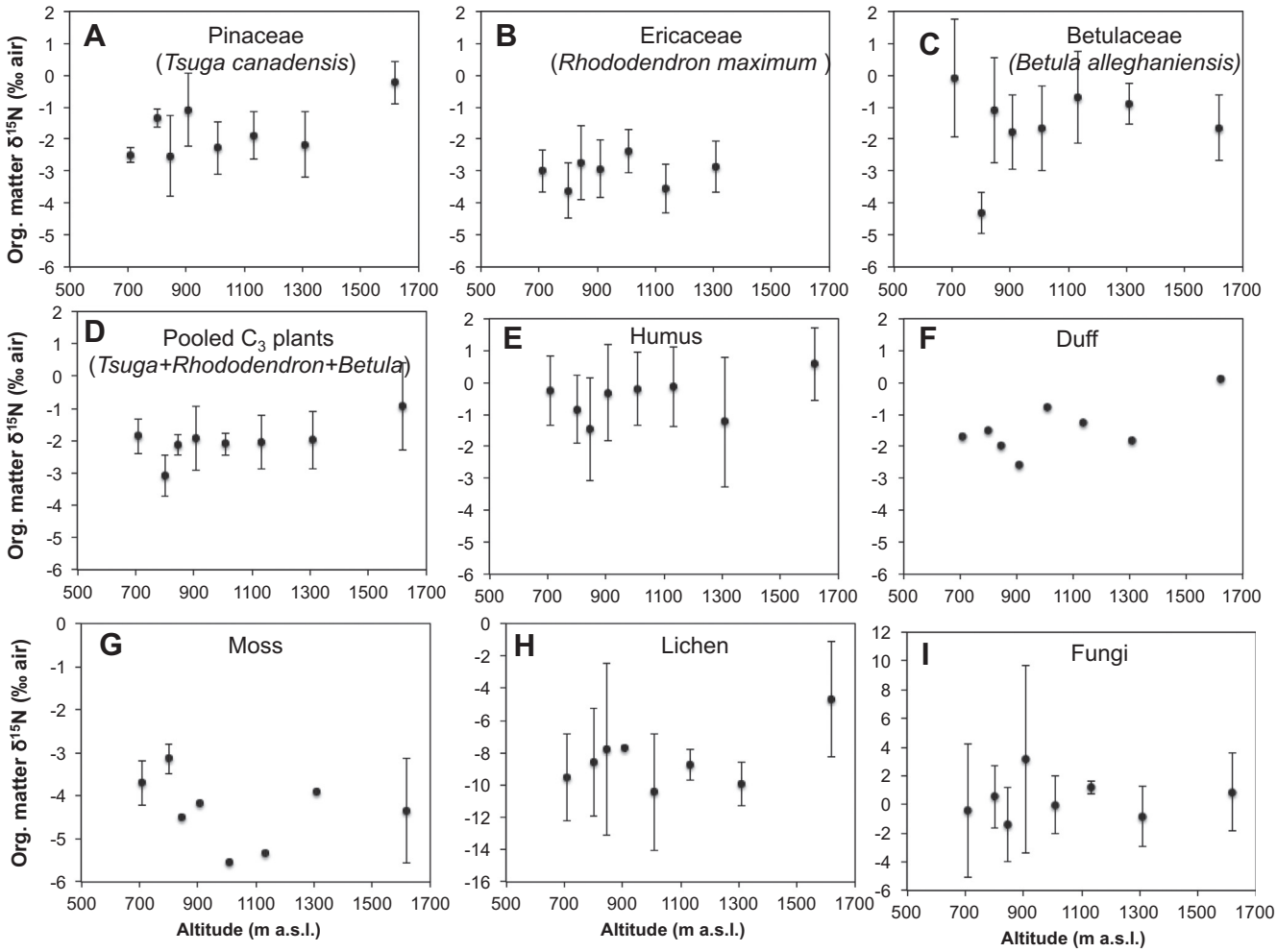

Fig. 5. Nitrogen stable isotopes of food resources along an altitudinal gradient in the Big Santeetlah Creek watershed. (A) $\delta^{15}N$ of *Tsuga canadensis*. (B) $\delta^{15}N$ of *Betula alleghaniensis*. (C) $\delta^{15}N$ of *Rhododendron maximum*. (D) $\delta^{15}N$ of pooled C_3 plants. (E) $\delta^{15}N$ of humus. (F) $\delta^{15}N$ of duff. (G) $\delta^{15}N$ of moss. (H) $\delta^{15}N$ of lichen. (I) $\delta^{15}N$ of fungi. Note that y-axes differ in panels G, H, and I.

sites varied from +1.8‰ to +5.7‰, with a mean value of +3.9 ± 1.2‰. Site-averaged $\Delta^{13}C_{shell\ org.-plant}$ varied from 1.2‰ to 5.0‰, and exhibited a mean value of +3.4 ± 1.3‰. On the other hand, the site-averaged $\Delta^{13}C_{body-shell\ org.}$ ranged from +0.2‰ to +0.7‰, with a mean value of +0.4 ± 0.3‰.

The $\delta^{15}N$ of snail body ranged from +0.4‰ to +4.9‰ (Table S3), and exhibited a mean value of +1.7 ± 1.0‰. Body $\delta^{15}N$ did not show a trend with altitude (Table 2; Fig. 7A), but samples from lower sites (< 1100 m) showed relatively higher values and exhibited a wider variance than samples from higher locales (> 1100 m). This pattern could potentially be explained by wetter/cooler conditions in higher altitude sites, which would lower the vegetation $\delta^{15}N$ (Handley et al. 1999). A similar trend was observed in the $\delta^{15}N$ of shell organics (Table S3), which ranged from +0.0‰ to +3.4‰, with a mean value of +1.1 ± 0.8‰ (Table 2; Fig. 7B). There was no trend in the $\delta^{15}N$ of body or shell organics with altitude (Fig. 7A-B). The nitrogen isotopic offset between snail body and C_3 plant ($\Delta^{15}N_{body-plant}$) ranged from +1.9‰ to +4.2‰, with a mean value of +3.4 ± 0.7‰ (Fig. 7C). Site-averaged $\Delta^{15}N_{shell\ org.-plant}$ varied from +1.6‰ to +3.3‰, with a mean value of +3.3 ± 1.6‰, whereas site-averaged $\Delta^{15}N_{body-shell\ org.}$ varied from +0.3‰ to +1.4‰, showing a mean value of +0.6 ± 0.4‰. $\delta^{15}N$ of snail body and shell organics was uncorrelated with the site-averaged $\delta^{15}N$ for food resources. The site-averaged $\delta^{15}N$ of body and shell organics correlated positively (Spearman correlation: $r_s = 0.94$, $p = 0.004$; $n = 7$) if the values from the Graves' Campsite at 845 m are omitted. Finally, $\delta^{13}C$ and $\delta^{15}N$ were uncorrelated for both body and shell organics (Table 2).

3.5. Shell carbonate $\delta^{13}C$

The $\delta^{13}C$ of the shell carbonate ranged from −15.2‰ to −7.3‰ (Table S3), showed a mean value of −11.2 ± 1.6‰, and did not vary with altitude (Fig. 6C). Shell $\delta^{13}C$ was uncorrelated with $\delta^{13}C$ of food resources by site. While raw data of shell $\delta^{13}C$ significantly correlated with $\delta^{13}C$ of body and shell organics, site-averaged shell $\delta^{13}C$ values were uncorrelated with values of both variables (Fig. 6E, F). The carbon isotopic offset between snail shell carbonate and C_3 plants ($\Delta^{13}C_{shell\ carb.-plant}$) varied from +15.7‰ to +20.0‰, with a mean value of +17.9 ± 1.2‰. The $\Delta^{13}C_{shell\ carb.-body}$ ranged from +9.8‰ to +17.6‰, with a mean value of +14.1 ± 1.7‰. The $\Delta^{13}C_{shell\ org.-shell\ carb.}$ Varied from +10.4‰ to +17.9‰ and displayed a mean value of +14.5 ± 1.6‰. Calculations from the flux balance-mixing model by Balakrishnan and Yapp (2004) for $\delta^{13}C$ indicate snails precipitated shell material with similar input and output flux of bicarbonate from the body fluid (near $\Phi = 0.00$) (Fig. 8).

4. Discussion and conclusions

4.1. Shell $\delta^{18}O$ as a paleoprecipitation proxy

The $\delta^{18}O$ of snail shell carbonate declined with increasing altitude at the rate of −0.06‰ per 100 m (Fig. 2B). This lapse rate is consistent

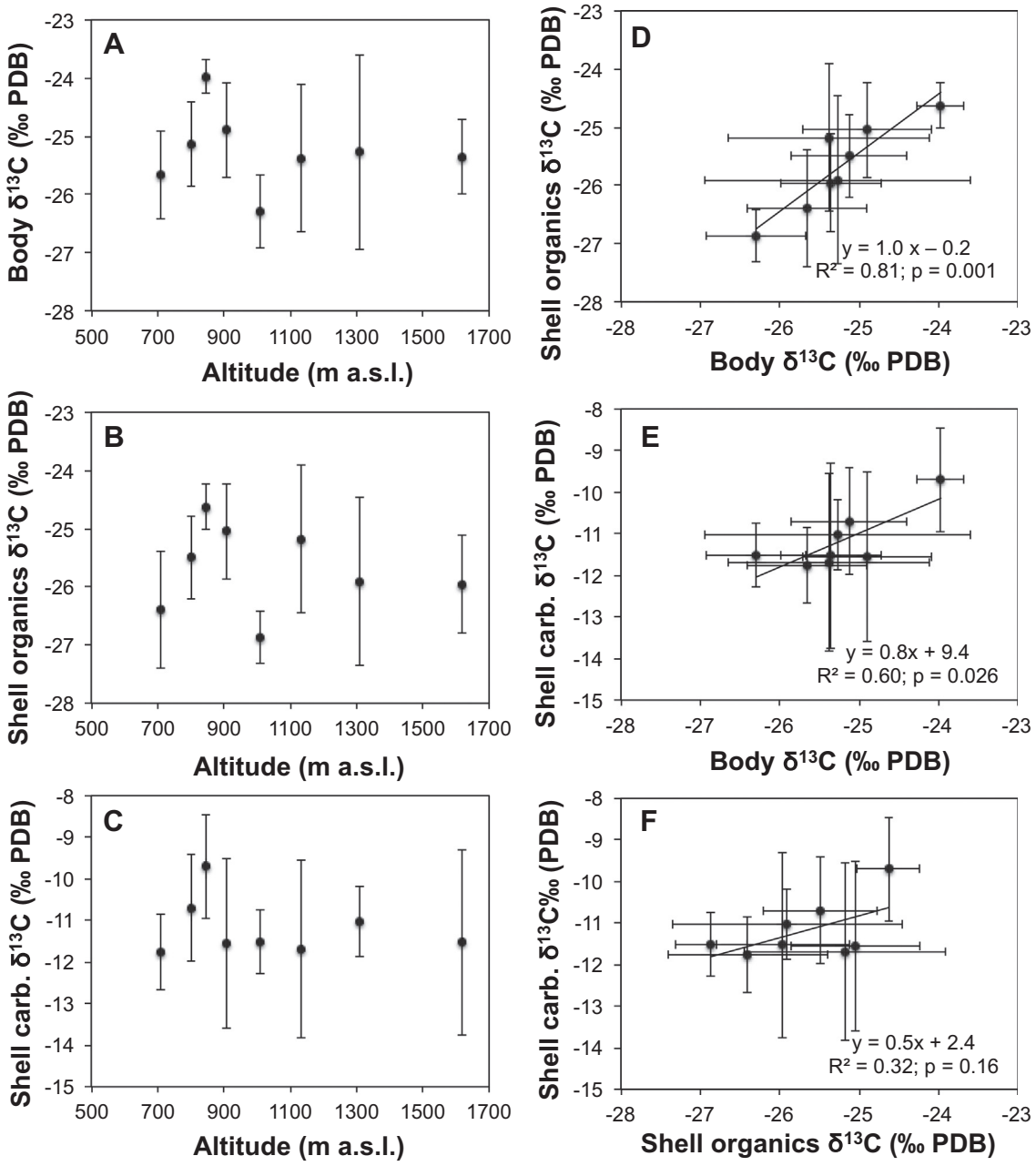

Fig. 6. Snail $\delta^{13}C$ along an altitudinal gradient in the Big Santeetlah Creek watershed. (A) Bulk body $\delta^{13}C$. (B) Bulk $\delta^{13}C$ of shell organic matrix. (C) Shell carbonate $\delta^{13}C$. (D) Relationship between site-averaged $\delta^{13}C$ of body and shell organics. (E) Relationship between site-averaged $\delta^{13}C$ of shell carbonate and body. (F) Relationship between site-averaged $\delta^{13}C$ of shell carbonate and shell organics.

with previous snail data sets from the southern Great Plains of North America (Balakrishnan et al. 2005a), Libya (Prendergast et al. 2015) and Tenerife Island of the Canary Archipelago (Yanes et al. 2009). This trend is best explained by the decline in precipitation $\delta^{18}O$ with increasing altitude (− 0.07‰ per 100 m; Fig. 2A), which in turn varies as a function of decreasing ambient temperature (e.g., Poage and Chamberlain, 2001; Bowman and Wilkinson, 2002). Site-averaged $\delta^{18}O$ for shell carbonate significantly correlated with measured rain $\delta^{18}O$ (Fig. 2C), in agreement with previous field studies using modern snails (e.g., Lécolle, 1985; Zanchetta et al. 2005; Yanes et al. 2008, 2009; Prendergast et al. 2015). Patterns of isotopic variance across sites in the Big Santeetlah Creek watershed suggests that the magnitude of intra- and inter-annual environmental fluctuations was similar across sampling locales during periods of snail shell calcification. The mean isotopic variation of shell $\delta^{18}O$ observed within localities in our study area (~2‰) was lower than the documented dispersion of ~3–5‰ in drier locales, such as the Canary Islands (e.g., Yanes et al. 2009). Lower variability in shell $\delta^{18}O$ values within sites in the Big Santeetlah Creek watershed likely reflects lower variability in environmental water $\delta^{18}O$ and reduced evaporation in humid Appalachian forests (e.g., Yanes et al. 2009).

The observed offset in $\delta^{18}O$ between shell and ambient water ($\Delta^{18}O_{shell\ carb\text{-}rain}$ of ~4‰) in the study area is in accord with previously published studies which have reported offsets between shell and ambient water as large as ~12‰ (Yapp, 1979; Goodfriend and Magaritz, 1987). The offset is likely caused by the enrichment of ^{18}O in snail body fluid through water loss to evaporation during calcification (Balakrishnan and Yapp, 2004).

Collectively, our results indicate that the $\delta^{18}O$ values of *Neohelix* shells from the Big Santeetlah Creek watershed appear to be affected

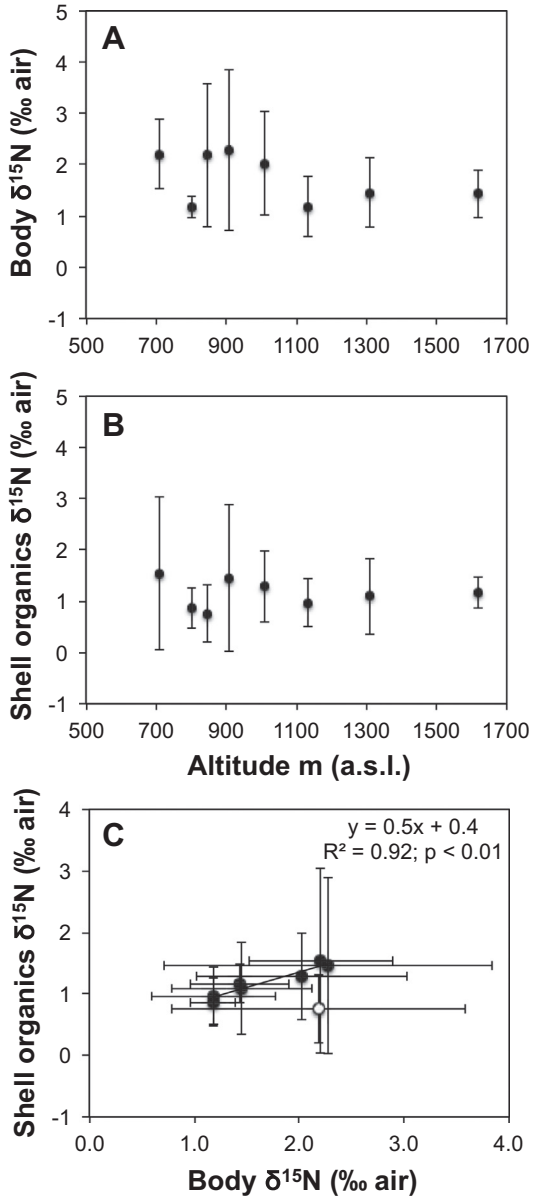

Fig. 7. Snail $\delta^{15}N$ along an altitudinal gradient in the Big Santeetlah Creek watershed. (A) Bulk body $\delta^{15}N$. (B) Bulk $\delta^{15}N$ of shell organic matrix. (C) Relationship between site-averaged $\delta^{15}N$ of snail body and shell organics. Note that Graves Camp site (white dot in panel C) was omitted because it was considered an outlier.

primarily by precipitation $\delta^{18}O$ during periods of shell growth. Fossil shelly assemblages of this species in North America should function reasonably well as a paleoclimatic indicator of meteoric water $\delta^{18}O$ values.

4.2. Shell $\delta^{13}C$ of *Neohelix major* morphotype as a paleovegetation proxy

Calculations from the flux balance mixing model indicate that land snails displayed little variation in metabolic rates along the altitudinal gradient in the Big Santeetlah Creek watershed (Fig. 8). These data suggest that variation in $\delta^{13}C$ of snail tissues are affected more by diet than differences in metabolic rate. Roughly 74–95% of the snail shell carbon derives from respired CO_2 (Stott, 2002), The observed isotopic fractionation of ~8 to ~19‰ between shell and organic tissue is expected due, in part, to the loss of isotopically lighter CO_2 molecules during respiratory gas exchange (McConnaughey and Gillikin, 2008). The carbon stable isotope fractionation between shell carbonate and

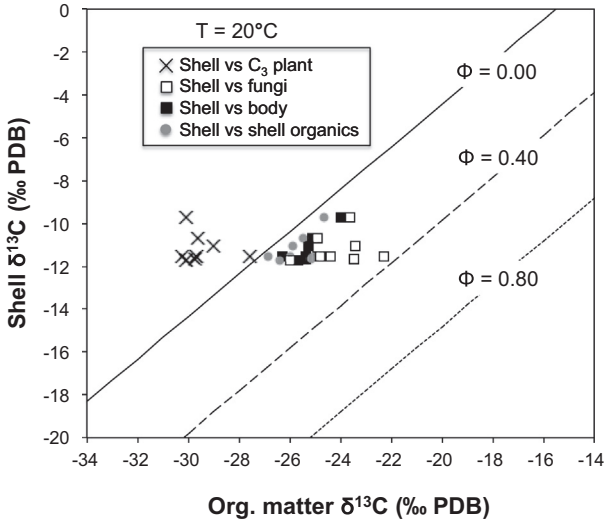

Fig. 8. Calculations of shell $\delta^{13}C$ using the snail evaporative steady-state flux balance model of Balakrishnan and Yapp (2004), assuming an ambient mean temperature of 20 °C. Note that other choices of temperatures do not significantly change model calculations.

snail organic tissue (~14‰) reported in this study is comparable to results of previously published studies for other large snail species (e.g., Stott, 2002; Metref et al. 2003; Yanes et al. 2008, 2013c; Prendergast et al. 2017).

Site-averaged shell $\delta^{13}C$ did not correlate with body and shell organics $\delta^{13}C$ (Fig. 6E–F). This suggests that even though snail shell $\delta^{13}C$ should primarily reflect the $\delta^{13}C$ of the snail organic tissues, which in turn records the signature of the consumed and assimilated foods, other factors are at work. Some field studies have shown that snails may ingest significant amounts of inorganic carbon from carbonate bedrock as a source of calcium to build their shells (e.g., Goodfriend, 1987; Goodfriend and Hood, 1983; Goodfriend et al. 1999; Yanes et al. 2008, 2013c). However, carbonate rocks are rare to absent in the Big Santeetlah Creek watershed, and therefore, limestone ingestion seems to be an unlikely cause of the apparent mismatch between the $\delta^{13}C$ of shell and organic tissues. Additionally, some studies have suggested that shell $\delta^{13}C$ can also be impacted by atmospheric CO_2 (Liu et al. 2007; McConnaughey and Gillikin, 2008) and perhaps, this may be the case for *Neohelix*. All in all, the present work indicates that additional research is needed to further understand the environmental significance of shell $\delta^{13}C$ in forested ecosystems. Future research on land snail foraging ecology should (1) investigate $\delta^{13}C$ and $\delta^{15}N$ profiles of a wider range of potential food resources (e.g., decayed animal matter, insects, wood ash, etc.), (2) analyze multiple syntopic snail species with possible differing ecological habits (e.g., microsnails versus large snails), and (3) consider complementary field observations, gut content analysis, and/or feeding laboratory experiments.

4.3. Assessing the foraging ecology of *Neohelix major* morphotype

The majority of land snail species are considered generalized herbivores that consume plants indiscriminately in relation to their abundance in the landscape (Speiser, 2001). $\delta^{13}C$ and $\delta^{15}N$ values of soft body tissues of *Neohelix* living in the Big Santeetlah Creek watershed in the Appalachian Mountains are comparable to those of snails classified as primary consumers (herbivores) and omnivores or microbe feeders in a tropical forest in Hawaii (Meyer and Yeung, 2011). We compared *Neohelix* values to those of potential dietary items, including C_3 plants, non-vascular plants (moss), decayed organic matter (duff and humus), lichens, and fungi (Fig. 9). *IsoSource* model outputs suggest that snails fed primarily on fungi (~48 ± 6% of the diet), followed by lichen (~17 ± 3%), humus (~11 ± 16%), duff (~10 ± 14%), moss

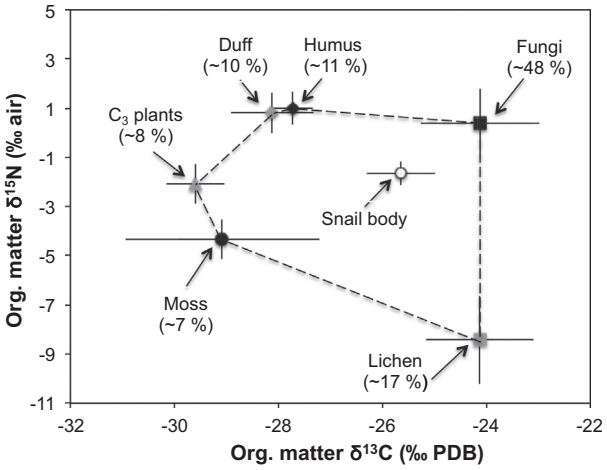

Fig. 9. Assessment of the foraging ecology of the land snail *Neohelix major* morphotype from the Big Santeetlah Creek watershed. Numbers between brackets depict *Isosource* outputs indicating possible relative average contributions of food items to snail's diet.

(~8 ± 7%) and C_3 plants (~7 ± 11%). Surprisingly, fresh C_3 plants appear to constitute a minor component of *Neohelix* diet, which suggests that Appalachian land snails may have more complex diets than anticipated. Other field studies have reported fungi as an important part of land snail diets (e.g., Dourson, 2008; Meyer and Yeung, 2011) and a laboratory experiment showed that some species preferred fungi over plant tissue (Pusledník, 2002).

Our results suggest that multi-isotope analyses of snails and their potential food sources offer significant insight on snail diets. Investigators should not overlook the need to understand modern land snail foraging ecology before interpreting shell $\delta^{13}C$ from fossil or archeological specimens.

Acknowledgments

This work was supported by the research grant NSF-EAR-1529133 to YY and the Alexander Wetmore Fund, Smithsonian Institution to GRG. GRG acknowledges the continuing support of the Smoketree Trust. Special thanks go to Barry Roth (University of California, Berkeley) who kindly identified the land snail taxon used in this study. Additional thanks go to Crayton J. Yapp (SMU) for providing insightful comments on earlier versions of this manuscript. The constructive and detailed revisions by Timothy Pearce (Carnegie Museum of Natural History) and an anonymous reviewer greatly improved the quality and clarity of this study.

Appendix A. Supplementary data

Supplementary data to this article can be found online at https://doi.org/10.1016/j.palaeo.2017.12.015.

References

Balakrishnan, M., Yapp, C.J., 2004. Flux balance model for the oxygen and carbon isotope compositions of land snail shells. Geochim. Cosmochim. Ac. 68, 2007–2024.
Balakrishnan, M., Yapp, C.J., Theler, J.L., Carter, B.J., Wyckoff, D.G., 2005a. Environmental significance of $^{13}C/^{12}C$ and $^{18}O/^{16}O$ ratios of modern land-snail shells from the southern Great Plains of North America. Quat. Res. 63, 15–30.
Balakrishnan, M., Yapp, C.J., Meltzer, D.J., Theler, J.L., 2005b. Paleoenvironment of the Folsom archaeological site, New Mexico, USA, approximately 10,500 ^{14}C yr B.P. as inferred from the stable isotope composition of fossil land snail shells. Quat. Res. 63, 31–44.
Baldini, L.M., Walker, S.E., Bruce, R., Baldini, J.U.L., Crowe, D.E., 2007. Isotope ecology of the modern land snails Cerion, San Salvador, Bahamas: preliminary advances toward establishing a low-latitude island palaeoenvironmental proxy. PALAIOS 22, 174–187.
Barrow, L.M., Bjorndal, K.A., Reich, K.J., 2008. Effects of preservation method on stable carbon and nitrogen isotope values. Physiol. Biochem. Zool. 81, 688–693.
Bolstad, P.V., Swift, L., Collins, F., Regniere, J., 1998. Measured and predicted air temperatures at basin to regional scales in the southern Appalachian Mountains. Agric. For. Meteorol. 91, 161–176.
Bowman, G.J., Wilkinson, B., 2002. Spatial distribution of ^{18}O in meteoric precipitation. Geology 30, 315–318.
Colonese, A.C., Zanchetta, G., Fallick, A.E., Martini, F., Manganelli, G., Lo Vetro, D., 2007. Stable isotope composition of late glacial land snail shells from Grotta del Romito (Southern Italy): paleoclimatic implications. Palaeogeogr. Palaeoclimatol. Palaeoecol. 254, 550–560.
Colonese, A.C., Zanchetta, G., Fallick, A.E., Martini, F., Manganelli, G., Russell, D., 2010a. Stable isotope composition of *Helix ligata* (Müller, 1774) from late Pleistocene-Holocene archaeological record from Grotta della Serratura (Southern Italy): paleoclimatic implications. Glob. Planet. Chang. 71, 249–257.
Colonese, A.C., Zanchetta, G., Dotsika, E., Drysdale, R.N., Fallick, A.E., Grifoni-Cremonesi, R., Manganelli, G., 2010b. Early-middle Holocene land snail shell stable isotope record from Grotta di Latronico 3 (southern Italy). J. Quat. Sci. 25, 1347–1359.
Colonese, A.C., Zanchetta, G., Russell, D., Fallick, A., Manganelli, G., Lo Vetro, D., Martini, F., di Giuseppe, Z., 2011. Stable isotope composition of late PleistoceneeHolocene *Eobania vermiculata* shells (Müller, 1774) (Pulmonata, Stylommatophora) from the central Mediterranean basin: data from Grotta d'Oriente (Favignana, Sicily). Quat. Int. 244, 76–87.
Cook, A., 2001. Behavioural ecology: on doing the right thing, in the right place at the right time. In: Barker, G.M. (Ed.), The Biology of Terrestrial Mollusk. CABI, pp. 447–487.
DeNiro, M.J., Epstein, S., 1978. Influence of diet on the distribution of carbon isotopes in animals. Geochim. Cosmochim. Ac. 42, 495–506.
Dourson, D.C., 2008. The feeding behavior and diet of an endemic West Virginia land snail, *Triodopsis platysayoides*. Am. Malacol. Bull. 26, 153–159.
Emberton, K.C., 1988. The genitalic, allozymic, and conchological evolution of the eastern North American Triodopsinae (Gastropoda: Pulmonata: Polygyridae). Malacologia 28, 159–273.
Emberton, K.C., 1995. Sympatric convergence and environmental correlation between two land-snail species. Evolution 49, 469–475.
Goodfriend, G.A., 1987. Radiocarbon age anomalies in shell carbonate of land snails from semi-arid areas. Radiocarbon 29, 159–167.
Goodfriend, G.A., 1988. Mid-Holocene rainfall in the Negev Desert from ^{13}C of land snail shell organic matter. Nature 333, 757–760.
Goodfriend, G.A., 1991. Holocene trends in ^{18}O in land snail shells from the Negev Desert and their implications for changes in rainfall source areas. Quat. Res. 35, 417–426.
Goodfriend, G.A., 1999. Radiocarbon age anomalies in land snail shells from Texas: ontogenetic, individual, and geographic patterns of variation. Radiocarbon 41, 149–156.
Goodfriend, G.A., Ellis, G.L., 2000. Stable carbon isotope record of middle to late Holocene climate changes from land snail shells at Hinds Cave, Texas. Quat. Int. 67, 47–60.
Goodfriend, G.A., Ellis, G.L., 2002. Stable carbon and oxygen isotope variations in modern *Rabdotus* land snail shells in the southern Great Plains, USA, and their relation to environment. Geochim. Cosmochim. Ac. 66, 1987–2002.
Goodfriend, G.A., Hood, D.G., 1983. Carbon isotope analysis of land snail shells: implications for carbon sources and radiocarbon dating. Radiocarbon 25, 810–830.
Goodfriend, G.A., Magaritz, M., 1987. Carbon and oxygen isotope composition of shell carbonate of desert land snails. Earth Planet. Sc. Lett. 86, 377–388.
Goodfriend, G.A., Ellis, G.L., Toolin, L.J., 1999. Radiocarbon age anomalies in land snail shells from texas: ontogenetic, individual and geographic patterns of variation. Radiocarbon 41, 149–156.
Graves, G.R., Romanek, C.S., 2009. Mesoscale patterns of altitudinal tenancy in migratory wood warblers inferred from stable carbon isotopes. Ecol. Appl. 19, 1264–1275.
Graves, G.R., Romanek, C.S., Rodríguez-Navarro, A., 2002. Stable isotope signature of philopatry and dispersal in a migratory songbird. P. Natl. Acad. Sci. USA 99, 8096–8100.
Grossman, E.L., Ku, T.L., 1986. Oxygen and carbon isotope fractionation in biogenic aragonite. Chem. Geol. 59, 59–74.
Hammer, Ø., Harper, D.A.T., Ryan, P.D., 2001. PAST - PAlaeontological STatistics, ver. 1.89. Palae 4, 1–9.
Handley, L.L., Austin, A.T., Robinson, D., Scrimgeour, C.M., Raven, J.A., Heaton, T.H.E., Schmidt, S., Stewart, G.R., 1999. The ^{15}N natural abundance ($\delta^{15}N$) of ecosystem samples reflects measures of water availability. Aust. J. Plant Physiol. 2, 185–199.
Hobson, K.A., Gibbs, H.L., Gloutney, M.L., 1997. Preservation of blood and tissue samples for stable-carbon and stable-nitrogen isotope analysis. Can. J. Zool. 75, 1720–1723.
Kehrwald, N.M., McCoy, W.D., Thibeault, J., Burns, S.J., Oches, E.A., 2010. Paleoclimatic implications of the spatial patterns of modern and LGM European land-snail shell $\delta^{18}O$. Quat. Res. 74, 166–176.
Körner, Ch., Farquhar, G.D., Roksandic, Z., 1988. A global survey of carbon isotope discrimination in plants from high altitude. Oecologia 74, 623–632.
Lécolle, P., 1985. The oxygen isotope composition of land snail shells as a climatic indicator: applications to hydrogeology and paleoclimatology. Chem. Geol. 58, 157–181.
Liu, Z.X., Gu, Z.Y., Wu, N.Q., Xu, B., 2007. Diet control on carbon isotopic composition of land snail shell carbonate. Chin. Sci. Bull. 52, 388–394.
Lubell, D., 2005. Are land snails a signature for the Mesolithic-Neolithic transition? Documenta Praehistorica 31, 1–24.
McConnaughey, T.A., Gillikin, D.P., 2008. Carbon isotopes in mollusk shell carbonates. Geo-Marine Lett. 28, 287–299.
Metref, S., Rousseau, D.D., Bentaleb, I., Labonne, M., Vianey-Liaud, M., 2003. Study of the diet effect on $\delta^{13}C$ of shell carbonate of the land snail *Helix aspersa* in experimental

conditions. Earth Planet. Sc. Lett. 211, 381–393.
Meyer, W.M., Yeung, N.W., 2011. Trophic relationships among terrestrial molluscs in a Hawaiian rain forest: analysis of carbon and nitrogen isotopes. J. Trop. Ecol. 27, 441–445.
Newsome, S.D., Phillips, D.L., Culleton, B.J., Guilderson, T.P., Koch, P.L., 2004. Dietary reconstruction of an early to middle Holocene human population from the central California coast: insights from advanced stable isotope mixing models. J. Archaeol. Sci. 31, 1101–1115.
Phillips, D.L., Gregg, J.W., 2003. Source partitioning using stable isotopes: coping with too many sources. Oecologia 136, 261–269.
Phillips, D.L., Newsome, S.D., Gregg, J.W., 2015. Combining sources in stable isotope mixing models: alternative methods. Oecologia 144, 520–527.
Pigati, J.S., Rech, J.A., Nekola, J.C., 2010. Radiocarbon dating of small terrestrial gastropod shells in North America. Quat. Geochronol. 5, 519–532.
Poage, M.A., Chamberlain, C.P., 2001. Empirical relationships between elevation and the stable isotope composition of precipitation and surface waters: considerations for studies of paleoelevation change. Am. J. Sci. 301, 1–15.
Post, D.M., 2002. Using stable isotopes to estimate trophic position: models, methods, and assumptions. Ecology 83, 703–718.
Prendergast, A.L., Stevens, R.E., Barker, G.O., Connell, T.C., 2015. Oxygen isotope signatures from land snail (*Helix melanostoma*) shells and body fluid: proxies for reconstructing Mediterranean and North African rainfall. Chem. Geol. 409, 87–98.
Prendergast, A.L., Stevens, R.E., O'Connell, T.C., Hill, E.A., Hunt, C., Barker, G.W., 2016. A late Pleistocene refugium in Mediterranean North Africa? Palaeoenvironmental reconstruction from stable isotope analysis of land snail shells (Haua Fteah, Libya). Quat. Sci. Rev. 139, 94–109.
Prendergast, A.L., Stevens, R.E., Hill, E.A., Hunt, C., O'Connell, T.C., Barker, G.W., 2017. Carbon isotope signatures from land snail shells: implications for palaeovegetation reconstruction in the eastern Mediterranean. Quat. Int. 432, 48–57.
Puslednik, L., 2002. Dietary preferences of two species of *Meridolum* (Camaenidae: Eupulmonata: Mollusca) in southeastern Australia. Molluscan Research 22, 17–22.
Sarakinos, H.C., Johnson, M.L., Vander Zanden, M.J., 2002. A synthesis of tissue-preservation effects on carbon and nitrogen stable isotope signatures. Can. J. Zool. 80, 381–387.
Speiser, B., 2001. Food and feeding behavior. In: Barker, G.M. (Ed.), The 8iology of Terrestrial Mollusk. CABI, pp. 259–288.
Stott, L.D., 2002. The influence of diet on the $\delta^{13}C$ of shell carbon in the pulmonate snail *Helix aspersa*. Earth Planet. Sc. Lett. 195, 249–259.
Sweeting, C.J., Polunin, N.V.C., Jennings, S., 2004. Tissue and fixative dependent shifts of $\delta^{13}C$ and $\delta^{15}N$ in preserved ecological material. Rapid Commun. Mass Spectrom. 18, 2587–2592.
Yanes, Y., 2015. Stable isotope ecology of land snails from a high latitude site near Fairbanks, interior Alaska, USA. Quat. Res. 83, 588–595.
Yanes, Y., Delgado, A., Castillo, C., Alonso, M.R., Ibáñez, M., De la Nuez, J., Kowalewski, M., 2008. Stable isotope ($\delta^{18}O$, $\delta^{13}C$, and δD) signatures of recent terrestrial communities from a low-latitude, oceanic setting: endemic land snails, plants, rain, and carbonate sediments from the eastern Canary Islands. Chem. Geol. 249, 377–392.
Yanes, Y., Romanek, C.S., Delgado, A., Brant, H.A., Noakes, J.E., Alonso, M.R., Ibáñez, M., 2009. Oxygen and carbon stable isotopes of modern land snail shells as environmental indicators from a low-latitude oceanic island. Geochim. Cosmochim. Ac. 73, 4077–4099.
Yanes, Y., Yapp, C.J., Ibáñez, M., Alonso, M.R., De la Nuez, J., Quesada, M.L., Castillo, C., Delgado, A., 2011a. Pleistocene-Holocene environmental change in the Canary archipelago as inferred from stable isotopes of land snail shells. Quat. Res. 65, 658–669.
Yanes, Y., Romanek, C.S., Molina, F., Cámara, J.A., Delgado, A., 2011b. Holocene paleoenvironment (7,200–4,000 cal. years BP) of the Los Castillejos archaeological site (Southern Spain) as inferred from stable isotopes of land snail shells. Quat. Int. 244, 67–75.
Yanes, Y., Gutiérrez-Zugasti, I., Delgado, A., 2012. Late glacial-Holocene transition in northern Spain deduced from terrestrial gastropod shelly accumulations. Quat. Res. 78, 373–385.
Yanes, Y., Riquelme, J.A., Cámara, J.A., Delgado, A., 2013a. Stable isotope composition of middle to late Holocene land snail shells from the Marroquíes archeological site (Jaén, southern Spain): paleoenvironmental implications. Quat. Int. 302, 77–87.
Yanes, Y., Gómez-Puche, M., Esquembre-Bebia, M.A., Fernández-López-de-Pablo, J., 2013b. Younger dryas – early Holocene transition in southeastern Iberian peninsula: insights from land snail shell middens. J. Quat. Sci. 28, 777–788.
Yanes, Y., Asta, M., Ibáñez, M., Alonso, M.R., Romanek, C.S., 2013c. Paleoenvironmental implications of carbon stable isotope composition of land snail tissues. Quat. Res. 80, 596–605.
Yanes, Y., Izeta, A.D., Cattaneo, R., Costa, T., Gordillo, S., 2014. Holocene (~4.5–1.7 cal. kyr BP) paleoenvironmental conditions in central Argentina inferred from entire-shell and intra-shell stable isotope composition of terrestrial gastropods. The Holocene 24, 1193–1205.
Yapp, C.J., 1979. Oxygen and carbon isotope measurements of land snail shell carbonates. Geochim. Cosmochim. Ac. 43, 629–635.
Zanchetta, G., Leone, G., Fallick, A.E., Bonadonna, F.P., 2005. Oxygen isotope composition of living land snail shells: data from Italy. Palaeogeogr. Palaeoclimatol. Palaeoecol. 223, 20–33.